

*Proceedings of “Applications of Physics in Mechanical and Material Engineering” (APMME 2023)*

## Influence of the Spin Wave Stiffness Parameter in Amorphous Materials on Saturation Magnetisation Value

B. JEŻ<sup>a</sup>, M. NABIAŁEK<sup>b</sup>, P. POSTAWA<sup>a</sup>, J. GODNRO<sup>b</sup>,  
M.M.A.B. ABDULLAH<sup>c</sup>, S. WALTERS<sup>d</sup>,  
B. KOCZURKIEWICZ<sup>e</sup> AND N.I. MUHAMMAD NADZRI<sup>f,g</sup>

<sup>a</sup>*Department of Technology and Automation, Faculty of Mechanical Engineering and Computer Science, Czestochowa University of Technology, al. Armii Krajowej 19c, 42-200 Czestochowa, Poland*

<sup>b</sup>*Department of Physics, Faculty of Production Engineering and Materials Technology, Czestochowa University of Technology, al. Armii Krajowej 19, 42-200 Czestochowa, Poland*

<sup>c</sup>*Center of Excellence Geopolymer & Green Technology (CeGeoGTech), Faculty of Chemical Engineering Technology, Kampus Dragon, Kompleks Pusat Pengajian Jejawi 3, 02600 Arau, Perlis, Malaysia*

<sup>d</sup>*Advanced Engineering Centre, University of Brighton, BN2 4GJ, Brighton, United Kingdom*

<sup>e</sup>*The Institute of Plastic Working and Safety Engineering, Faculty of Production Engineering and Materials Technology, Czestochowa University of Technology, al. Armii Krajowej 19, 42-200 Czestochowa*

<sup>f</sup>*Center of Excellence Geopolymer and Green Technology, Universiti Malaysia Perlis, Taman Muhibbah, 02600 Arau, Perlis, Malaysia*

<sup>g</sup>*Faculty of Chemical Engineering and Technology, Universiti Malaysia Perlis, Taman Muhibbah, 02600 Arau, Perlis, Malaysia*

Doi: [10.12693/APhysPolA.144.375](https://doi.org/10.12693/APhysPolA.144.375)

\*e-mail: [barlomiej.jez@pcz.pl](mailto:barlomiej.jez@pcz.pl)

Depending on their other constituent elements, Fe-based amorphous materials can exhibit good soft magnetic properties. By determining the directional coefficient  $b$  for the relationship of  $\mu_0 M(\mu_0 H)^{1/2}$  according to the best linear fit, it is possible to determine the parameter of spin wave stiffness  $D_{spf}$ . This parameter, amongst others, is related to the distribution of magnetic atoms around the central atom, which is reflected in the value of saturation magnetisation. This work has examined the structure of specially prepared alloy samples and analysed the influence of the spin wave stiffness parameter on the value of saturation magnetisation. Three alloys with different constitutions, based on the Fe matrix, were analysed.

topics: amorphous alloys, primary magnetisation curve, saturation magnetisation, spin wave stiffness parameter

### 1. Introduction

Modern electronic and electrical components require increasingly improved materials that meet relevant requirements. A particular example is the magnetic cores used in all smartphones, tablets, computers and many other modern devices. The most suitable magnetic materials for this type of application are materials with soft magnetic properties [1–3], i.e., low remagnetisation losses, high magnetic permeability, and relatively high values of Curie temperature and saturation magnetisation. Limiting the losses per remagnetisation cycle helps to increase the efficiency of electrical devices, concurrently reducing the temperature and noise emission associated with their operation [4, 5].

In amorphous soft magnetic materials, the phenomenon of magnetostriction is significantly reduced, with some alloys containing cobalt reaching magnetostriction values close to zero (near-zero magnetostriction) [6, 7]. This phenomenon is widely known and manifests itself in a change in one or more dimensions of the material with changes in the direction of magnetisation. For decades, work has been carried out to reduce the phenomenon of magnetostriction in materials commercially used in the electrical energy and electronic industries. The Curie temperature is a very important parameter for characterising the operation of soft magnetic materials. This temperature sets a certain limit, determining the point of change of magnetic structure from ferromagnetic to paramagnetic [8]. This means

that above the Curie temperature, ferromagnetic properties are lost. Another important parameter for describing soft magnetic materials is saturation magnetisation; it determines the state of magnetic saturation, i.e., it describes the state at which an increase in the strength of an external magnetic field does not cause any further increase in the magnetisation of the material. In the case of the tested alloys, a state close to the saturation state is achieved in relatively low magnetic fields of about 1 T. Above that value, in strong magnetic fields, the magnetisation process and increase in magnetisation value are no longer associated with the presence of structural defects, and the main factor affecting the changes in magnetisation is that of spin waves. These waves are collectively induced spin systems. Systems of interacting spins are described in Heisenberg's model [9].

Using the relationship of  $\mu_0 M(\mu_0 H)^{1/2}$ , it is possible to determine the  $D_{spf}$  spin wave stiffness parameter associated with parameter  $b$ , which is described by the following formula [10]

$$b = 3.54g\mu_0\mu_B \left( \frac{1}{4\pi D_{spf}} \right)^{3/2} k_B T (g\mu_B)^{1/2}, \quad (1)$$

where:

- $\mu_0$  — magnetic permeability of a vacuum,
- $H$  — magnetic field,
- $k_B$  — Boltzmann's constant,
- $\mu_B$  — Bohr magneton,
- $g$  — gyromagnetic factor,
- $T$  — temperature.

This parameter is related to the number of nearest magnetic neighbours. The value of this parameter is directly related to the value of saturation magnetisation.

The aim of this research was to study the structure and to determine the parameter of spin wave stiffness for samples of the bulk amorphous alloy family —  $\text{Fe}_{65}\text{Nb}_5\text{Hf}_{5-x}\text{Y}_{5+x}\text{B}_{20}$  (where  $x = 0, 1$ , or  $2$ ). The tested samples were soft magnetic ferromagnets in the form of a plate with a thickness of 0.5 mm.

## 2. Materials and methods

The samples prepared for this research were made in two stages. The first stage consisted of weighing and melting the alloy component elements to obtain crystalline ingots. All the alloy components used at this stage were of high purity: Fe — 99.99 at.%, Nb — 99.99 at.%, Hf — 99.99 at.%, Y — 99.95 at.%, B — 99.9 at.%. The ingredients were melted on a copper water-cooled plate under a protective gas atmosphere. The polycrystalline ingots were remelted four times on each side to improve their homogeneity. Each melt was preceded by the melting of pure titanium, which was used as an absorbent of the

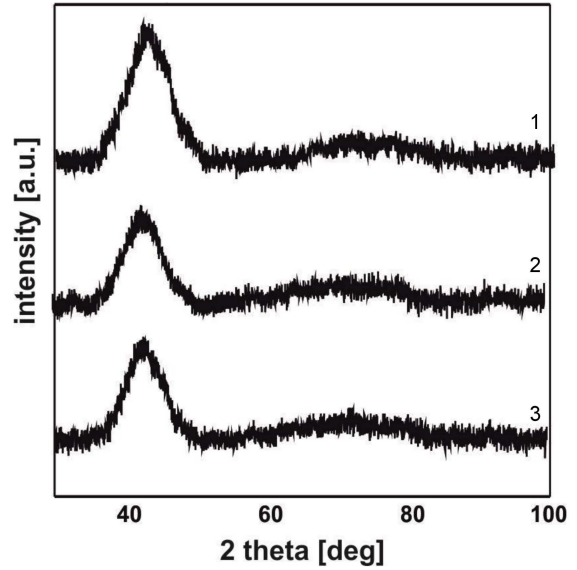


Fig. 1. X-ray diffraction patterns for the plate-form samples of the investigated alloys:  $\text{Fe}_{65}\text{Nb}_5\text{Hf}_5\text{Y}_5\text{B}_{20}$  (curve 1),  $\text{Fe}_{65}\text{Nb}_5\text{Hf}_4\text{Y}_6\text{B}_{20}$  (curve 2),  $\text{Fe}_{65}\text{Nb}_5\text{Hf}_3\text{Y}_7\text{B}_{20}$  (curve 3).

remaining oxygen in the chamber. The prepared alloy ingots were divided into smaller pieces, which were used to make rapidly cooled samples. The samples were produced in the form of plates with a thickness of 0.5 mm and an area of 100 mm<sup>2</sup> using an injection-casting method — the liquid alloy was forced, under argon pressure, into a copper water-cooled mould. The structure of the resulting samples was evaluated by means of a Bruker ADVANCE D8 X-ray diffractometer equipped with a cobalt lamp. The samples were tested over the range of  $2\theta$  angle from 30 to 100°, with an exposure time per measuring step of 5 s at a resolution of 0.02°. The magnetic properties of the samples were investigated using a Lakeshore 7307 vibrating sample magnetometer. Measurements of the primary magnetisation curves were carried out within the range of magnetic field strength of up to 2 T.

## 3. Results

Figure 1 shows the X-ray diffraction images measured for the tested alloys.

In the measured diffractograms, wide, fuzzy maxima (amorphous halos) are visible in the range of 40–55° of  $2\theta$  angle. These maxima are related to X-rays scattered on atoms randomly distributed in the volume of the alloy.

Figure 2 shows static magnetic hysteresis loops measured for the investigated alloys.

The measured loops for alloys with an yttrium content of 6 at.% and 7 at.% are similar to each other. The curve for  $\text{Fe}_{65}\text{Nb}_5\text{Hf}_5\text{Y}_5\text{B}_{20}$  is characterised by a different trajectory — the alloy

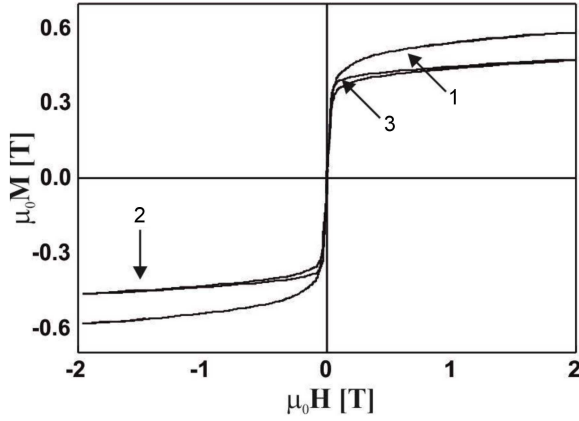


Fig. 2. Static magnetic hysteresis loops for the investigated alloys:  $\text{Fe}_{65}\text{Nb}_5\text{Hf}_5\text{Y}_5\text{B}_{20}$  (curve 1),  $\text{Fe}_{65}\text{Nb}_5\text{Hf}_4\text{Y}_6\text{B}_{20}$  (curve 2),  $\text{Fe}_{65}\text{Nb}_5\text{Hf}_3\text{Y}_7\text{B}_{20}$  (curve 3).

TABLE I

Magnetic properties of the investigated alloys.

Alloy	$M_S$ [T]	$H_C$ [A/m]	$H_{H-P}$ [T]	$D_{spf}$ [meV nm <sup>2</sup> ]
$\text{Fe}_{65}\text{Nb}_5\text{Hf}_5\text{Y}_5\text{B}_{20}$	0.58	189	0.43	27
$\text{Fe}_{65}\text{Nb}_5\text{Hf}_4\text{Y}_6\text{B}_{20}$	0.47	129	0.31	32
$\text{Fe}_{65}\text{Nb}_5\text{Hf}_3\text{Y}_7\text{B}_{20}$	0.47	42	0.13	38

reaches a much higher saturation magnetisation value. Figure 3 shows the magnetisation curves as a function of  $(\mu_0 H)^{1/2}$ .

A linear fit was made to the trajectory of the magnetisation as a function  $(\mu_0 H)^{1/2}$ . The parameter  $b$  and the magnitude of the external magnetic field, at which the magnetisation process of the alloy is associated with the so-called Holstein–Primakoff paraprocess (attenuation of thermally induced spin waves), were determined. Magnetic properties, based on the static magnetic hysteresis loops and magnetisation as a function of  $(\mu_0 H)^{1/2}$ , are shown in Table I.

Despite minor differences in the chemical composition of the alloys, their magnetic properties differ significantly. The addition of the Y element, at the expense of the Hf element, causes a significant decrease in the value of the coercivity field and the field at which the Holstein–Primakoff paraprocess begins. The alloy sample with 7 at.% of Y element exhibits a much easier magnetisation process. Moreover, it is worth noting that the value of the  $D_{spf}$  parameter increases with increasing addition of the Y element. As previously mentioned, this parameter is closely related to the number of nearest magnetic neighbours (Fe atoms) and thus to magnetisation. The increase in the value of the  $D_{spf}$  parameter is associated with changing distance between the Fe atoms. Given the simultaneous decrease in the value of saturation magnetisation, it can be con-

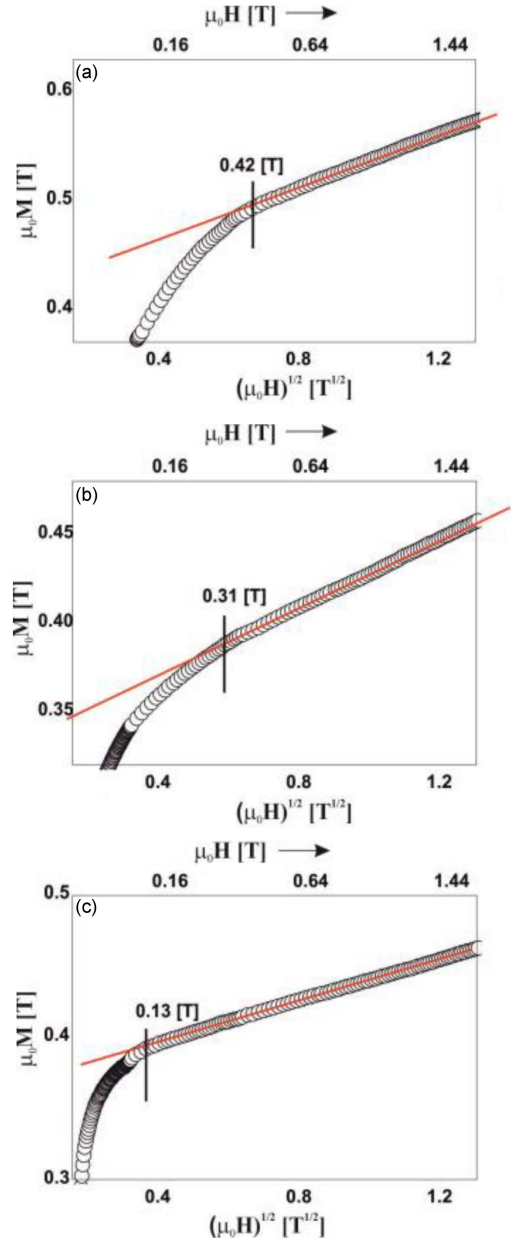


Fig. 3. Magnetisation as a function of  $(\mu_0 H)^{1/2}$  for the investigated alloys: (a)  $\text{Fe}_{65}\text{Nb}_5\text{Hf}_5\text{Y}_5\text{B}_{20}$ , (b)  $\text{Fe}_{65}\text{Nb}_5\text{Hf}_4\text{Y}_6\text{B}_{20}$ , (c)  $\text{Fe}_{65}\text{Nb}_5\text{Hf}_3\text{Y}_7\text{B}_{20}$ .

cluded that there is a local anti-ferromagnetic order in the tested samples. In some areas of the alloys, the Fe atoms are close enough to each other that they force anti-ferromagnetic spin alignment, which results in a decrease in the value of saturation magnetisation.

#### 4. Conclusions

This paper presents the results of research into the influence of Y and Hf element content on the structure and properties of bulk rapidly cooled alloys based on the Fe matrix. All the studied alloys

are characterised by an amorphous structure. Studies of the magnetic properties have shown that these alloys exhibit soft magnetic properties. It has been shown that the addition of the Y element at the expense of the Hf element affects the distribution of Fe atoms in the volume of the alloy — the distances between these atoms change. Therefore, there is an increase in the value of the  $D_{spf}$  parameter with a simultaneous decrease in the value of saturation magnetisation. This suggests the presence of local anti-ferromagnetic order in the volume of the alloys. Importantly, the existence of this magnetic order has no effect on the drastic increase in the value of the coercive field.

### References

- [1] X. Li, Z. Shi, T. Zhang, *J. Alloy. Compd.* **784**, 1139 (2019).
- [2] F. Wang, A. Inoue, Y. Han, F. Kong, S. Zhu, E. Shalaan, F. Al-Marzouki, A. Obaid, *J. Alloy. Compd.* **711**, 132 (2017).
- [3] M.E. McHenry, M.A. Willard, D.E. Laughlin, *Prog. Mater. Sci.* **44**, 291 (1999).
- [4] R. Piccin, P. Tiberto, H. Chiriac, M. Baricco, *J. Magn. Magn. Mater.* **320**, 806 (2008).
- [5] M. Nabiałek, S. Walters, K. Błoch, K. Jeż, M. Talar, M.A.A. Mohd Salleh, D.S. Che Halin, B. Jez, *Acta Phys. Pol. A* **139**, 503 (2021).
- [6] G. Herzer, *Acta Mater.* **61**, 718 (2013).
- [7] Y. Wu, T. Bitoh, K. Hono, A. Makino, A. Inoue, *Acta Mater.* **49**, 4069 (2001).
- [8] Z. Hou, J. Zhang, S. Xu, C. Wu, J. Zhang, Z. Wang, K. Yang, W. Wang, X. Dua, F. Su, *J. Magn. Magn. Mater.* **324**, 2771 (2012).
- [9] J. Coey, *Magnetism and Magnetic Materials*, Cambridge 2009.
- [10] T. Holstein, H. Primakoff, *Phys. Rev.* **58**, 1098 (1940).